Towards better description of gallo-phosphate materials in solid state NMR: 1D and 2D correlation studies

V. Montouillout, C. M. Morais, A. Douy, F. Fayon, D. Massiot

Towards a better description of gallo-phosphate materials in solid state NMR: 1D and 2D correlation studies

Valérie Montouillout*, Cláudia M. Morais†, André Douy, Franck Fayon and Dominique Massiot

CRMHT – CNRS UPR4212 1D, avenue de la Recherche Scientifique, 45071 Orléans cedex 2, France

Abstract

We show that weak $^{2}J(^{71}\text{Ga-O-}^{31}\text{P})$, typically ~12 Hz in $GaPO_4$, can be used to efficiently establish heteronuclear $^{31}\text{P-}^{71}\text{Ga}$ correlation using a MAS HMQC experiment in gallo-phosphate materials. The experiment demonstrated for cristobalite $GaPO_4$ is then applied to $Ga(PO_3)_3$ where it allows the differentiation of the signature of three different Ga sites overlapping in the 1D spectrum.

Keywords: NMR, ^{71}Ga, ^{31}P, HMQC experiment, gallo-phosphates.

1. Introduction

Molecular sieves based on metal phosphates have been subject to numerous investigations owing to their interesting structural chemistry and potential applications in catalysis, adsorption and ion exchange. After the successful synthesis of series of $AlPO_4$-*n* [1] alumino-phosphates, aluminium/gallium substitution, modifying acidic properties has also retained attention. High Resolution Solid State NMR has been a method of choice to assist X-ray or neutron diffraction in understanding the structure of many $AlPO_4$-*n* based materials, with experiments ranging from the simple 1D observation of ^{31}P or ^{27}Al to more sophisticated Multiple Quantum Magic Angle Spinning (MQMAS) for ^{27}Al [2], Homonuclear correlation of ^{31}P [3] or ^{27}Al (DQ-DCQ [4], H-HSQC [5]) or Heteronuclear correlation $^{31}\text{P}/^{27}\text{Al}$ (MQ-HETCOR [6, 7], *J*-HMQC [8], *J*-Resolved experiments [9]). These experiments allow probing the connectivity of the Al/O/P network as a function of distances using the through space dipolar interaction, or as a function of chemical bonding using the scalar part of the indirect *J*-coupling.

Recent years have shown the growth of another important family of molecular sieves or porous materials, the gallo-phosphate based materials. Some of these compounds adopt well known zeolitic framework topologies, but many of them exhibit novel structures. High resolution solid state gallium NMR, required for the characterization of these materials, remains little developed, mainly because of the large

* Correspondence to:
Valérie Montouillout, CRMHT-CNRS, 1D avenue de la Recherche Scientifique, 45071 Orléans cedex, France, tel/fax:33 2 38 25 55 11/ 33 2 38 63 81 03, email valerie.montouillout@cnrs-orleans.fr
† Now at Institut Lavoisier, Université de Versailles-Saint-Quentin-en-Yvelines, 78035 Versailles cedex, France

quadrupole momentum of the NMR observable isotopes of gallium, ^{69}Ga and ^{71}Ga (both I=3/2). This usually results in a very large second order quadrupolar broadening of their NMR spectra (typically several hundreds of kHz at the usual principal fields for ^{71}Ga and even more for ^{69}Ga), and in the unique observation of the central transition that can be manipulated as a fictitious spin I=1/2. With these large broadenings, MAS NMR of the central transition often gives very complex spectra with overlapping second order broadened spinning sidebands, and seldom succeeds in giving enhanced resolution. Even if sophisticated spin system manipulations can sort out these spinning sidebands to achieve ultimate resolution [10], the static spectrum of the central transition often remains the more informative spectrum at conventional principal fields (300 to 500 MHz) [11]. Due to the intense quadrupolar interaction, satellite transitions are difficult to observe and triple quantum coherence remains difficult to generate. Consequently MQ-MAS [12,13] or ST-MAS [14] experiments are difficult to implement efficiently. Similarly, spin locking of the severely broadened central transition, necessary for cross polarization [15,16] and HETCOR [17,18] experiments remains very difficult to implement (dependence of rf field strength, spinning rate, offset, …).

With the availability of high field solid state NMR spectrometers (750 MHz and over) combined with high speed magic angle spinning (30 kHz), this picture is modified because second order broadening diminishes with increasing field [19] and becomes comparable to achievable spinning rates [20]. Under these conditions, it becomes possible to acquire well-resolved spectra with a limited number of spinning sidebands and to extract reliable values of isotropic chemical shift, quadrupolar coupling constant, quadrupolar asymmetry parameter and intensity [21,22,23] for ^{71}Ga spectra.

In this contribution we show that, under high resolution MAS conditions at high field, it becomes possible to make use of the recently described HMQC experiment [24] to obtain heteronuclear ^{31}P/^{71}Ga correlation mediated by the scalar part of the indirect *J*-coupling $^{2}J(^{71}\text{Ga-O-}^{31}\text{P})$ that we estimate or measure for the first time. This experiment is directly characteristic of the ^{31}P-O-^{71}Ga chemical bond and provides detailed insight of the framework structure. We first demonstrate the approach with the case of $GaPO_4$ that involves one gallium and one phosphorus crystallographic site and then show that it can be applied to more complex crystalline gallo-phosphate systems with the example of $Ga(PO_3)_3$.

2. Experimental

2.1 Synthesis

Titrated aqueous solutions of gallium nitrate $Ga(NO_3)_3$ and ammonium dihydrogenophosphate $NH_4H_2PO_4$ (Aldrich) were mixed in the stoichiometric ratios, resulting into a clear solution for Ga:P and a milky solution for Ga:3P. These solutions were gelled by an auxiliary polyacrylamide gel [25] by addition of 6g of acrylamide and 1g of N,N'-methylenebisacrylamide as monomers dissolved in 100ml of the initial solutions. The gels were rapidly obtained after heating to 80-100°C with addition of a few drops of concentrated solution of α,α'-azoisobutyronitrile in acetone. The obtained gels were calcined at 5°C/min up to 700°C for 1h in a ventilated electric furnace, before grinding and further heating at 1300°C for 3h to obtain white powder samples. The

obtained powder of $GaPO_4$ revealed to be the single cristobalite $GaPO_4$ phase by XRD. After heating at 700°C for 15h, the phosphorous-rich sample crystallises into $Ga(PO_3)_3$ with a little amount of $GaPO_4$ as secondary phase and also a little amount of residual amorphous phase.

2.2 High resolution solid-state NMR

The ^{31}P high resolution solid state NMR experiments were conducted at 7.0 T on a Bruker Avance 300 spectrometer using a 4mm CP-MAS probehead. The ^{31}P quantitative MAS spectra were recorded at a spinning frequency of 15 kHz using a (π/8) pulse and a recycle delay of 360 s to obtain a quantitative spectrum. The ^{31}P two-dimensional (2D) homonuclear through-bond correlation spectra were acquired using the refocused INADEQUATE pulse sequence [26]. The delays for the double-quantum excitation and reconversion were synchronized with the rotor period. The ^{31}P nutation frequency was 90 kHz. The recycle delay was set to 30 s and a presaturation sequence was applied to ensure equivalent conditions for each transient.

The ^{71}Ga and ^{71}Ga-^{31}P double-resonance NMR experiments were performed at 17.6 T on a Bruker Avance 750 spectrometer equipped with a triple resonance 4 mm MAS probe. The spinning rate was fixed to 15 kHz. The ^{71}Ga MAS spectra were acquired using a rotor-synchronized Hahn-echo sequence and a low radio-frequency field strength to ensure a selective excitation of the central transition (ν_{RF} = 20 kHz). Similar ^{71}Ga selective excitation conditions were also used for the measurements of the transverse relaxation time T_2' and for the ^{71}Ga-^{31}P double-resonance experiments. The ^{71}Ga-^{31}P heteronuclear through-bond correlation MAS spectra were recorded using the HMQC sequence [8] at a spinning frequency of 15 kHz. The delays used for the heteronuclear multiple-quantum excitation and reconversion were synchronized with the rotor period and the ^{31}P nutation frequency was 45 kHz. For ^{71}Ga echo and ^{71}Ga-^{31}P HMQC experiments, the recycling delay was set to 1s. The ^{71}Ga and ^{31}P chemical shifts were referenced relative to $Ga(NO_3)_3$ 1M and 85% H_3PO_4 solutions, respectively.

3. Results and Discussion

3.1. $GaPO_4$ cristobalite

$GaPO_4$, as $AlPO_4$ compounds, can crystallize in polymorphic forms related to the SiO_2 polymorphs. Our synthesis and heating treatment lead to the formation of the cristobalite $GaPO_4$ form consisting in alternating GaO_4 and PO_4 tetrahedra. Both gallium and phosphorus atoms occupy a single crystallographic site. The ^{71}Ga MAS spectrum of $GaPO_4$ cristobalite, shown in figure 1(a1), exhibits a unique resonance with a typical second-order quadrupolar line-shape. This signal can be well simulated using the isotropic chemical shift and quadrupolar interaction parameters (δ_{CS} = 116 ppm, C_Q = 4.7 MHz and η_Q = 0.45) in agreement with previously published data [21] and confirming that gallium occupies a single tetrahedral site. The ^{31}P MAS NMR spectrum consists in a single resonance (δ_{CS} = -8.9 ppm, FWHM = 155 Hz) corresponding also to a single crystallographic site. Attempts to increase resolution by application of ^{71}Ga continuous wave decoupling led no significant effect. This is in contrast with what was observed with ^{27}Al decoupling of ^{31}P MAS spectra of crystalline alumino-phosphates

[27]. In fact the situation in gallo-phosphate is more complex because of the existence of two gallium isotopes (^{69}Ga - I = 3/2 - 60,4% abundant and ^{71}Ga - I = 3/2 - 39.6% abundant) and of large quadrupolar interaction affecting the satellite transitions, that cannot be efficiently irradiated. It is more than likely that ^{71}Ga cw irradiation could only decouple the central transition thus leading no significant sharpening of the ^{31}P line dominated by the coupling with ^{69}Ga and the outer transitions of ^{71}Ga.

As in the case of alumino-phosphate the existence of significant scalar part of the indirect *J*-coupling $^2J(^{71}\text{Ga-O-}^{31}\text{P})$, non vanishing under magic angle spinning, can be evidenced using the *J*-Resolved experiment [8]. A spin echo experiment, carried out at 15 kHz, leads a single exponential T'_2 relaxation time (coherence life time) [28] of 18.5 ms. Application of a π pulse on the ^{31}P channel simultaneously with the ^{71}Ga π pulse of the echo sequence introduces a modulation by the *J*-coupling with the four neighbouring ^{31}P coupled sites (figure 2). The *J*-resolved decay can be satisfactorily modelled considering the measured echo T'_2 and a single value of 12 Hz for the $^2J(^{71}\text{Ga-O-}^{31}\text{P})$ scalar *J*-coupling. If we consider this value of 12 Hz for $^2J(^{71}\text{Ga-O-}^{31}\text{P})$ (~15 Hz for $^2J(^{69}\text{Ga-O-}^{31}\text{P})$), the total *J* broadening of the ^{31}P line would be a quintuplet (coupling to 4 ^{69,71}Ga) of quartet (coupling to I=3/2 ^{69,71}Ga) consistent with the 155 Hz line-width observed in the ^{31}P spectrum. The difference signal between the echo decay and the *J*-resolved decay is the build up curve of the ^{71}Ga-^{31}P HMQC signal. This value is significantly lower than the $^2J(^{27}\text{Al-O-}^{31}\text{P})$ constants in $AlPO_4$ berlinite measured at 19.5 and 26 Hz [8].

As shown in figure 2(c), the $^2J(^{71}\text{Ga-O-}^{31}\text{P})$ scalar *J*-coupling is weak (12Hz) but significant and leads a ~20% transfer efficiency in the HMQC experiment for a τ delay (excitation and reconversion) of 9.3 ms. An equivalent experiment could be built starting from ^{31}P excitation, detecting the ^{71}Ga in the indirect dimension but would greatly suffer from the very long T_1 relaxation time of ^{31}P. In addition, because ^{71}Ga signal remains broad and thus decays rapidly, it is possible to acquire the full echo improving the signal to noise ratio by up to a factor of $2^{1/2}$ and providing unambiguous phasing to obtain a pure absorption spectrum [11]. Figure 1 shows the ^{71}Ga-^{31}P MAS HMQC spectrum of $GaPO_4$. As expected, the spectrum consists in a single correlation peak between the gallium and phosphorus resonances. The ^{71}Ga projection of the 2D experiment superimposes with the 1D MAS spectrum and the modelled line-shape, indicating homogeneous excitation of the powdered sample. For this sample the efficiency of the experiment is such that the spectrum of figure 1 has been obtained in ~35 minutes.

3.2. Gallium tris(metaphosphate) $Ga(PO_3)_3$

As previously mentioned, our phosphorous-rich sample, noted Ga:3P, contains mostly crystallised $Ga(PO_3)_3$ but also little amounts of low crystallized $GaPO_4$ and of a residual amorphous phase. The structure of $Ga(PO_3)_3$, previously described by Anisimova et al. [29] involves three Ga and nine P inequivalent crystallographic sites. In this structure, the phosphorus occupy tetrahedrally coordinated positions $P(OP)_2(OGa)_2$ leading to infinite phosphate chains. These chains are separated by gallium atoms occupying octahedrally coordinated positions $Ga(OP)_6$.

Figure 3(a) shows the ^{71}Ga spectrum of the Ga:3P sample. The line at 109.5 ppm is obviously attributed to tetra-coordinated Ga site in $GaPO_4$ cristobalite. In contrast with the case of the previous sample, the asymmetric line-shape of its ^{71}Ga resonance (sharp low field and trailing high field edge) is characteristic of a poorly organized

structure resulting from the low heating temperature, i.e. 700°C. The main line is centred on -70 ppm and exhibits several spinning sidebands. Its position is characteristic of 6-fold coordinated gallium. Its broad asymmetric line-shape arises from the overlap of the signatures of the different Ga sites and including a distribution of the quadrupolar interaction. We determine a global T_2' relaxation time (coherence life time) [28] integrating the total intensity of the main line. This value is estimated to typically 17 ms at 15 kHz. However, as this main line seems to be the sum of several overlapping contributions, the T_2' value of each contribution could be slightly different.

The ^{31}P MAS NMR spectrum of the sample is presented in figure 3(b). It consists of 7 main lines with maxima ranging from -35 to -55 ppm, ascribed to $Ga(PO_3)_3$ and an additional resonance (δ_{CS} = - 10.8 ppm, FWHM = 258 Hz) attributed to the phosphorus site of cristobalite $GaPO_4$. The main lines of the spectrum can be simulated with 7 lines (table 1), with relative intensities in the ratio 1:1:2:1:1:2:1 corresponding to the nine crystallographically inequivalent phosphorus sites of the structure. However the assignment of these numerous resonances can not be done on the base of this single 1D experiment. To go further and identify the chemically bonded pairs of ^{31}P we used a 2D refocused INADEQUATE experiment that allows to probe the P-O-P connectivity scheme in crystalline and disordered phosphates [30]. The ^{31}P 2D homonuclear correlation spectra (sheared and symmetrised) obtained at 10 and 15 kHz are shown in figure 4. In both spectra, each P resonance exhibits two resolved cross-correlation peaks, except for the two P resonances of double intensity which show correlation with at least three distinct P sites. These cross-peaks reflect the through-bond $^2J(^{31}$P-O-P) couplings expected from the proposed structure which involve infinite phosphate chains. Interestingly, the 2D refocused INADEQUATE spectrum obtained at 10 kHz shows several additional auto-correlation peaks of weak intensities, which disappear in the 2D spectrum obtained at higher spinning frequency. According to a recent work, these unexpected auto-correlation peaks can be attributed to the specific case of a homonuclear dipole-dipole coupled spin-pair with identical isotropic chemical shift but anisotropic chemical shift tensors with different magnitudes or principal orientations (non-zero DD-CSA cross terms) [31] and reflect the through-space proximities between crystallographically equivalent P sites having different orientation in the structure. The magnitude of these auto-correlation peaks is expected to decrease when increasing the spinning frequency as experimentally observed in the spectrum obtained at 15 kHz.

As shown above in the case of cristobalite $GaPO_4$, the ^{71}Ga-^{31}P HMQC experiment can be used to probe the through-bond Ga-O-P connectivity allowing a complete description of the $Ga(PO_3)_3$ framework. The $Ga(PO_3)_3$ part of this experiment is shown in figure 5, excluding the $GaPO_4$ correlation signal. The efficiency of the experiment, and thus the intensity of the $^2J(^{71}$Ga-O-^{31}P) scalar coupling (seen in the build up of the HMQC signal) clearly varies from site to site. It remains weak for the ^{31}P resonances ranging from – 44 to - 55 ppm which thus may undergo smaller $^2J(^{71}$Ga-O-^{31}P) couplings. The simulations of the different resolved cross-correlation peaks were conducted using a physically relevant model, with an interplay of a gaussian distribution of isotropic chemical shift and a distribution of quadrupolar coupling [32, 33]. They indicate that different ^{31}P lines are correlated to three distinguished ^{71}Ga sites that can now be identified in the four projections of figure 5(c1-4), and that correspond to the

three hexa-coordinated gallium sites described in the crystalline structure [29]. These three resonances can not be well-simulated using the same NMR parameters, which indicates unambiguously that the broad ^{71}Ga 1D spectrum is composed of three distinct contributions: Ga(1): δ_{iso} = -61.3ppm, C_Q = 6.4MHz - Ga(2): δ_{iso} = -68.6ppm, C_Q = 2.8MHz and Ga(3): δ_{iso} = -64.2ppm, C_Q = 4.5MHz (cf table 2). Therefore, this HMQC experiment allows the separation of the three different Ga sites from their linked ^{31}P signatures.

4. Conclusion

We show that weak unresolved $^2J(^{71}\text{Ga-O-}^{31}\text{P})$ of ~12 Hz in $GaPO_4$ can be used to efficiently establish heteronuclear $^{31}\text{P}/^{71}\text{Ga}$ correlation using a MAS HMQC experiment. The *J*-couplings in gallo-phosphate appear to be smaller that those observed in equivalent alumino-phosphate and to strongly depend on the nature of the chemical bond. The $^{71}\text{Ga-}^{31}\text{P}$ MAS HMQC experiment, first demonstrated on the case of cristobalite $GaPO_4$ can apply to more complex gallo-phosphate structures, providing separation of overlapping ^{71}Ga lines and detailed insight to the structure of $Ga(PO_3)_3$ identifying the different structural motifs.

Acknowledgements

We acknowledge financial support from CNRS UPR4212, FR2950, Region Centre and Ministère de la Recherche, and CNRS Post-Doc fellowship for CM.

References

1 S.T. Wilson, B.M. Lok, C.A. Messina, T.R. Cannan, E.M. Flanigen, *J. Am. Chem. Soc.* 1982; **104**: 1146-1147.

2 C. Fernandez, J.P. Amoureux, J.M. Chézeau, L. Delmotte, H. Kessler, *Micropor. Mater.* 1996; **6**:331-340.

3 M. Roux, C. Marichal, J.M. Le Meins, C. Baerlocher, J.M. Chézeau, *Micropor. Mesopor. Mater.* 2003; **63**, 163-176.

4 G. Mali, F. Taulelle**,** *Chem. Commun*. 2004: 868-869.

5 M. Deschamps, F. Fayon, V. Montouillout, D. Massiot, *accepted in Chem. Commun. DOI*

6 C. Fernandez, C. Morais, J. Rocha, M. Pruski, *Solid State NMR* 2001; **21:** 61-70.

7 J.W. Wiench, M. Pruski, *Solid State NMR* 2004; **26**: 51-55.

8 D. Massiot, F. Fayon, B. Alonso, J. Trebosc, J.P. Amoureux, *J. Magn. Reson.* 2003; **164**: 165-170.

9 J.P. Amoureux, J. Trebosc, J.W. Wiench, D. Massiot, M. Pruski, *Solid State NMR* 2005; **27:** 228-232.

10 D. Massiot, V. Montouillout, F. Fayon, P. Florian, C. Bessada, *Chem. Phys. Lett.* 1997; **272:** 295-300.

11 D. Massiot, I. Farnan, N. Gautier, D. Trumeau, A. Trokiner, J.P. Coutures, *Solid State NMR* 1995; **4:** *241-248*.
12 L. Frydman, J.S. Harwood, *J. Am. Chem. Soc.* 1995; **117**: 5367-5368.
13 A. Medek, J.S. Harwood, L. Frydman, *J. Am. Chem. Soc.* 1995; **117**: 12779-12787.
14 Z. Gan, *J. Am. Chem. Soc.* 2000; **122**: 3242-3243.
15 Vega A.J., *J. Magn. Res*. 1992; **96**: 50-68
16 Vega A.J., *J. Solid State NMR*. 1992; **1**: 17-32
17 C. A. Fyfe, H. Grondey, K.T. Mueller, K.C. Wong-Moon, T. Markus, *J. Am. Chem. Soc.* 1992; **114**: 5876-5878.
18 C. A. Fyfe, K.T. Mueller, H. Grondey, K.C. Wong-Moon, *J. Phys. Chem.* 1993; **97**: 13484-13495.
19 Z. Gan, P. Gor'kov, T.A. Cross, A. Samoson, D. Massiot *J. Am. Chem. Soc.* 2002; **124:** *5634-5635*.
20 M. Bujoli-Doeuff, M. Evain, P. Janvier, D. Massiot, A. Clearfield, Z. Gan, B. Bujoli, *Inorg. Chem.* 2001; **40:** *6694-6698*.
21 D. Massiot, T. Vosegaard, N. Magneron, D. Trumeau, V. Montouillout, P. Berthet, T. Loiseau, B. Bujoli, *Solid State NMR* 1999; **15**: 159-169.
22 D. Massiot, V. Montouillout, C. Magnenet, C. Bessada, J.P. Coutures, H. Forster, S. Steuernagel, D. Mueller *C. R. Acad. Sci. Paris* série IIC 1998; **1**: 157-162.
23 J.-C. Lavalley, M. Daturi, V. Montouillout, G. Clet, C. Otera Areán, M. Rodríguez Delgado, A. Sahibed-dine, *Phys. Chem. Chem. Phys.* 2003; **5**: 1301-1305.
24 A. Lesage, D. Sakellariou, S. Steuernagel, L. Emsley, *J. Am. Chem. Soc.* 1998; **120**: 13194-13201.
25 A. Douy, *Intern. J. Inorg. Mat.* 2001, **3:** 699-707.
26 A. Lesage, M. Bardet, L. Emsley, *J. Am. Chem. Soc.* 1999; **121**: 10987-10993.
27 L. Delevoye, C. Fernandez, C. M. Morais, J. P. Amoureux, V. Montouillout, J. Rocha, *Solid State NMR* 2002; **22:** 501-512.
28 S.P. Brown, M. Perez-Torralba, D. Sanz, R.M. Claramunt, L. Emsley, *Chem. Commun.* 2002: 1852-1853.
29 N. Anisimova, R. Glaum, *Z. Anorg. Allg. Chem.* 1998; 624: 2029-2032.
30 F. Fayon, G. Le Saout, L. Emsley, D. Massiot, *Chem. Commun.* 2002:1702-1703.
31 F. Fayon, D. Massiot, M. Levitt, J.J. Titman, D.H. Gregory, L. Duma, L. Emsley, S. Brown, *J. Chem. Phys*. 2005; **122**: 194313-194326.
32 D. Massiot, F. Fayon, M. Capron, I. King, S. Le Calvé, B. Alonso, J-O. Durand, B. Bujoli, Z. Gan, G. Hoatson, *Magn. Reson. Chem.* 2002; **40**: 70-76.
33 D. R. Neuville, L. Cormier and D. Massiot, *Geochimica et Cosmochimica Act* 2004*;* **68**, N^{o} 24: 5071–5079.

	P(1)	P(2)	P(3)	P(4)	P(5)	P(6)	P(7)
δ_{iso}(ppm)	-38.1	-40.5	-45.6	-46.7	-48.3	-48.9	-51.13
FWHM (Hz)	272	378	215	316	249	309	226
multiplicity	1	1	2	1	1	2	1

Table 1: ^{31}P NMR parameters of $Ga(PO_3)_3$ compound

	Ga(1)	Ga(2)	Ga(3)
δ_{iso}(ppm)	-61.3	-68.6	-64.2
C_Q(MHz)	6.4	2.8	4.5

Table 2: ^{71}Ga NMR parameters of $Ga(PO_3)_3$ compound: average isotropic chemical shift, δ_{iso}, and quadrupolar coupling constant, C_Q. These values are obtained by the simulation of the experimental spectra using a model which interplay a gaussian distribution of δ_{iso} and a distribution of C_Q [32; 33]. In this model, the quarupolar asymmetry parameter η_Q is fixed at 0.61

Figures captions

Figure 1: ^{71}Ga-^{31}P MAS HMQC spectrum of $GaPO_4$ (B_0 = 17.6T, ν_R=15kHz, $\tau_{excitation}$ = $\tau_{reconversion}$ = 9 ms, 264 t_1 slices and 16 scans) experimental time ~35mn (a1) the ^{71}Ga 1D MAS spectrum, (a2) the ^{71}Ga HMQC projection (a3) the modelled lineshape, (b1) the ^{31}P 1D MAS spectrum, (b2) the ^{31}P HMQC projection.

Figure 2: $\{^{31}P\}^{71}$Ga *J*-resolved experiment on GaPO4 acquired at 15kHz (a) decay of the ^{71}Ga spin echo signal (no ^{31}P pulse), (b) decay of the $\{^{31}P\}^{71}$Ga *J*-resolved signal (c) build-up of ^{71}Ga - ^{31}P HMQC signal. The symbols correspond to experimental data, and the continuous line to their modelling assuming a mono exponential decay for the echo (T_2'=18.5ms) and a 12 Hz $^2J(^{71}Ga\text{-}O\text{-}^{31}P)$ coupling to four ^{31}P for the *J*-resolved experiment.

Figure 3: ^{71}Ga MAS (a) and ^{31}P MAS (b) spectra of Ga:3P sample (B_0 = 17.6T, ν_R=15kHz).

Figure 4: ^{31}P-^{31}P refocused INADEQUATE spectra, sheared and symmetrized (B_0 = 7T, 78 t_1 slices, 16 scans, $\tau_{excitation}$ = $\tau_{reconversion}$ = 3.7ms) acquired with a spinning frequency of 10 kHz (a) and 15 kHz (b). (a1) and (b1) correspond to extracted slices from 10 kHz and 15 kHz spectra respectively.

Figure 5: ^{71}Ga-^{31}P MAS HMQC spectrum of $(GaPO_3)_3$ compound (B_0 = 17.6T, ν_R=15kHz, $\tau_{excitation}$ = $\tau_{reconversion}$ = 5.3 ms, 168 t_1 slices and 928 scans) (a1) the ^{71}Ga 1D MAS spectrum, (a2) the ^{71}Ga HMQC projection, (b1) the ^{31}P 1D MAS spectrum, (b2) the ^{31}P HMQC projection. c(1-4) correspond to ^{71}Ga extracted slices, full lines are experimental spectra and dot lines calculated spectra.

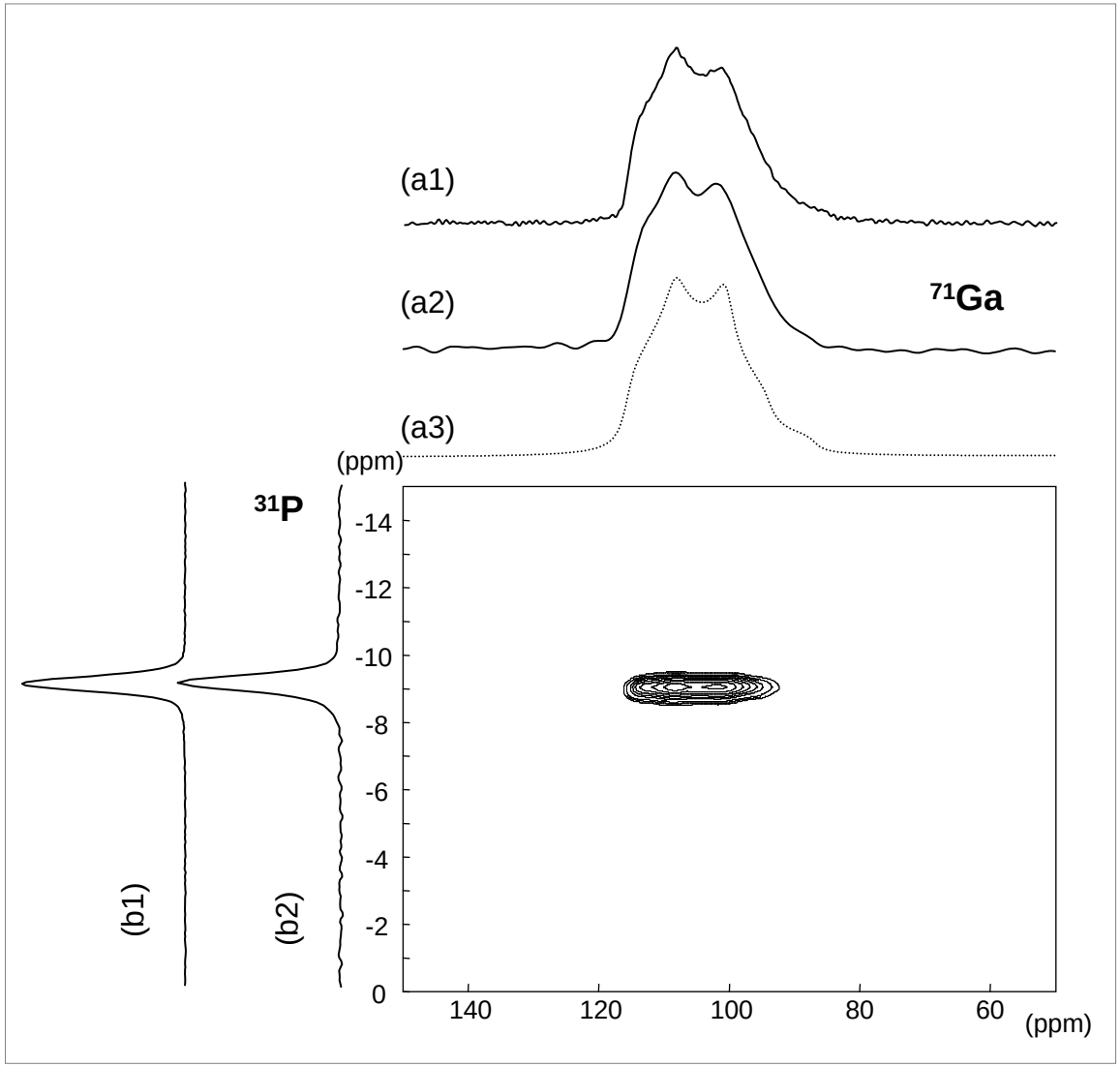

V. Montouillout

Figure 1

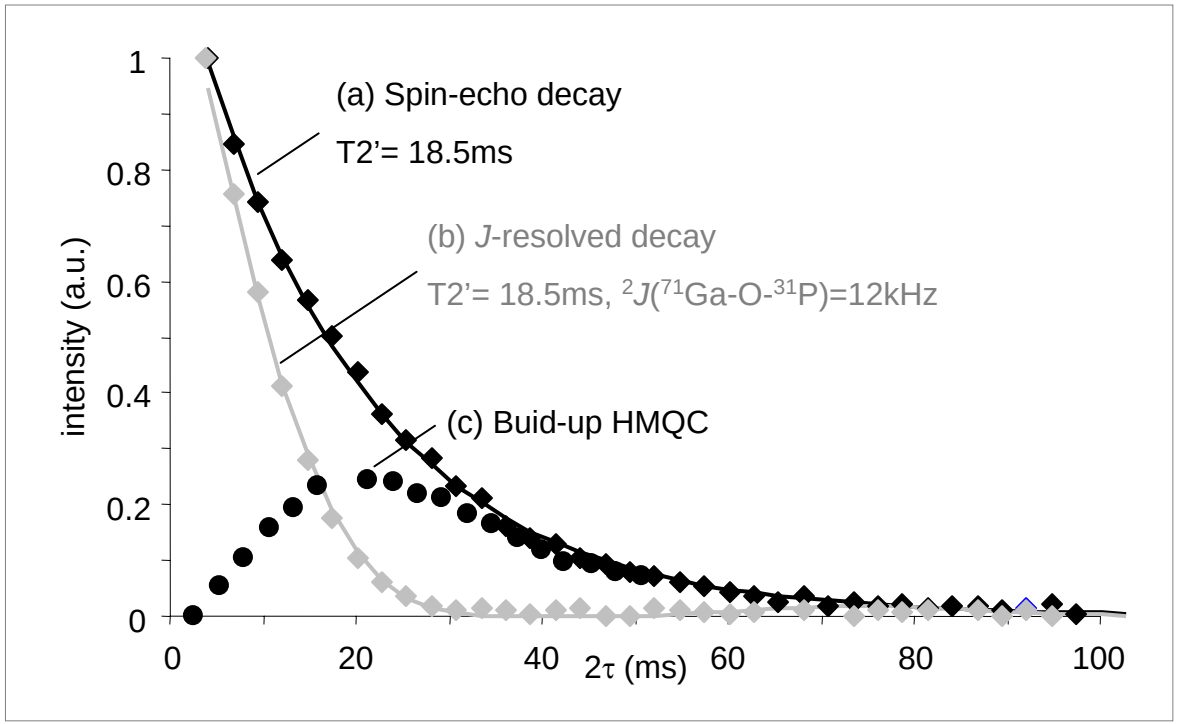

V. Montouillout

Figure 2

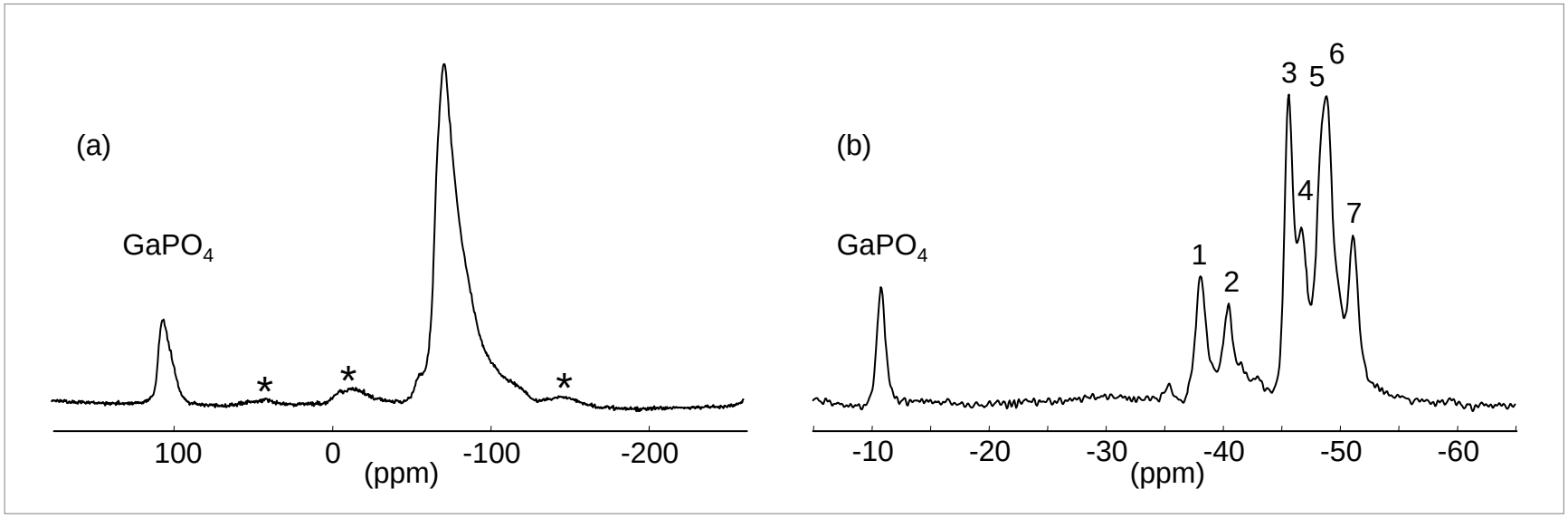

V. Montouillout

Figure 3

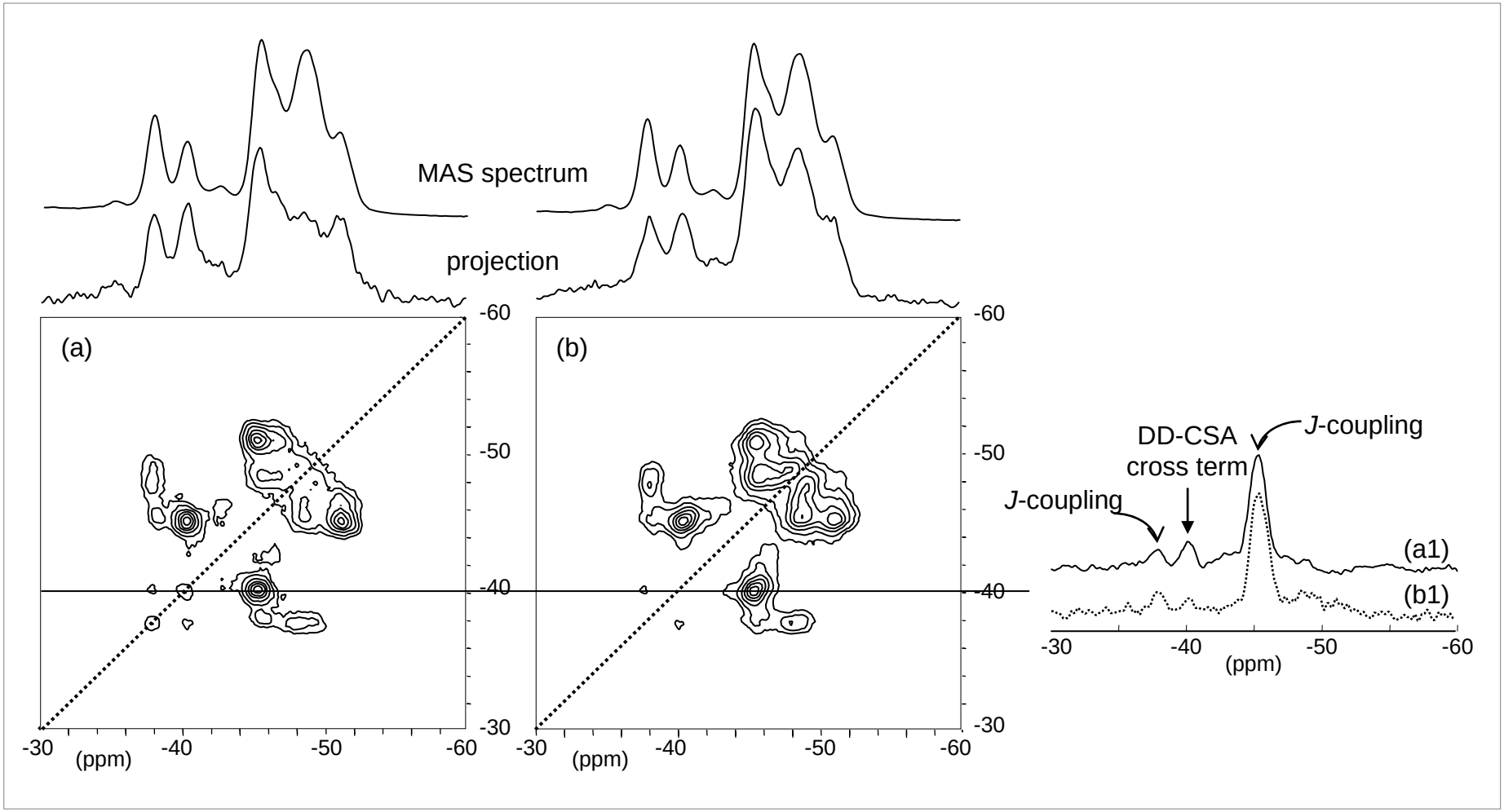

V. Montouillout

Figure 4

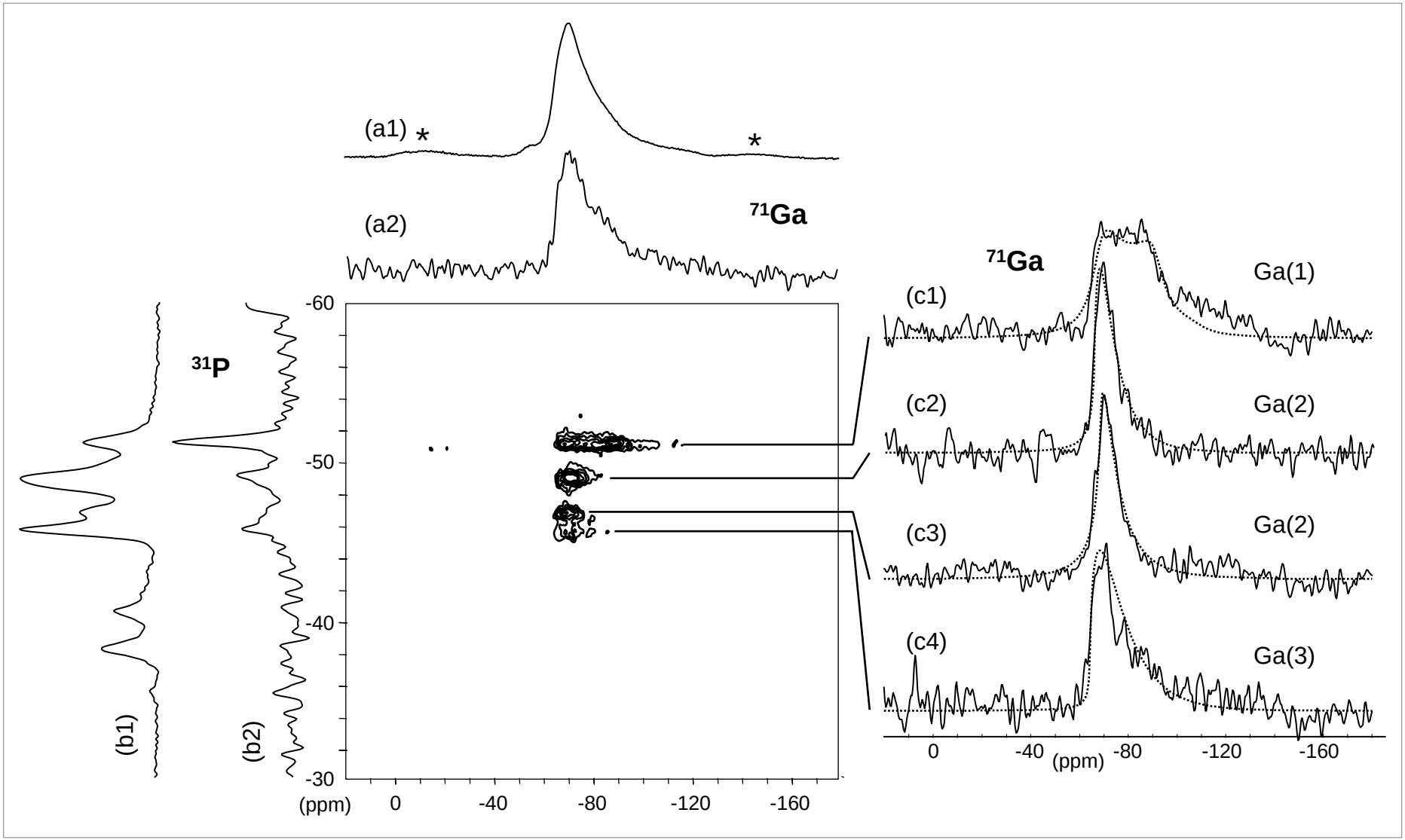

V. Montouillout

Figure 5